JOURNAL OF PETROLOGY | VOLUME 42 | NUMBER 1 | PAGES 131–140 | 2001

Emplacement of Deep Upper-Mantle Rocks into Cratonic Lithosphere by Convection and Diapiric Upwelling

M. R. DRURY[1]*, H. L. M. VAN ROERMUND[1], D. A. CARSWELL[2], J. H. DE SMET[1], A. P. VAN DEN BERG[1] AND N. J. VLAAR[1]

[1]VENING MEINESZ RESEARCH SCHOOL OF GEODYNAMICS, FACULTY OF EARTH SCIENCES, UTRECHT UNIVERSITY, PO BOX 80·021, 3508 TA UTRECHT, NETHERLANDS

[2]ENVIRONMENTAL AND GEOLOGICAL SCIENCES, UNIVERSITY OF SHEFFIELD, DAINTON BUILDING, BROOKHILL, SHEFFIELD S3 7HF, UK

RECEIVED DECEMBER 17, 1999; REVISED TYPESCRIPT ACCEPTED JUNE 26, 2000

*Rocks containing breakdown products of majoritic garnet, derived from the deep upper mantle, occur in kimberlite xenoliths and in orogenic peridotites from Otrøy in Norway. The Otrøy peridotites are banded harzburgites and dunites with similar compositions to mantle xenoliths from Precambrian cratons and Phanerozoic supra-subduction-zone peridotites. Pressure–temperature (*P–T*) paths deduced for the Otrøy peridotites and kimberlite xenoliths from South Africa are consistent with emplacement of deep mantle peridotites into cratonic lithosphere by asthenosphere diapirism. Numerical thermo-convection models provide insight into the possible* P–T *histories of deep upper-mantle rocks. In the models, material from the base of the convecting system is transported to depths of 60–100 km by convection and small (50–100 km) diapirs. Diapir intrusion induces small-scale convection in the low-viscosity deeper part of the thermochemically defined lithosphere. Small-scale convection in the craton root can produce complex* P–T *paths, complex recurrent melting histories and complex compositional structure in the craton.* P–T *paths derived from the numerical models for asthenosphere diapirism in a hot upper mantle are consistent with the sequence of sub-solidus* P–T *conditions deduced for the cratonic peridotites.*

KEY WORDS: *asthenosphere diapirs; cratonic lithosphere; deep upper mantle; majoritic garnet*

INTRODUCTION

Some mantle xenoliths (Haggerty & Sautter, 1990) and diamond inclusion suites (Moore & Gurney, 1985; Moore *et al.*, 1991) are derived from the deep upper mantle (150–410 km), transition zone (410–670 km) (Sautter *et al.*, 1991) and even the lower mantle (Scott-Smith *et al.*, 1984; Kesson & Fitz Gerald, 1991; Harte *et al.*, 1999). A few orogenic peridotite bodies may also be derived from the deep upper mantle (Pearson *et al.*, 1989; Dobrzhinetskaya *et al.*, 1996; Van Roermund & Drury, 1998; Bozhilov *et al.*, 1999), although some cases are controversial (Pfiffner *et al.*, 1998; Bozhilov *et al.*, 1999).

Peridotites from the deep upper mantle probably consist of olivine, clinopyroxene and majoritic garnet (Herzberg, 1995). Majoritic garnet has Si in tetrahedral and octahedral sites. Octahedral co-ordination for Si is significant only above 4·5 GPa (at 1200°C) and the amount of Si increases with pressure. If majoritic garnet is decompressed it breaks down to garnet with pyroxene exsolution. Breakdown products of majoritic garnet were first found in kimberlite xenoliths by Haggerty & Sautter (1990) and similar relict microstructures have recently been found in orogenic peridotites from the Western Gneiss Region (WGR) in Norway (Van Roermund & Drury, 1998; Terry *et al.*, 1999).

In this contribution we consider the role of asthenosphere diapirism in the emplacement of deep upper-mantle peridotites into the cratonic lithosphere. The

*Corresponding author. Telephone: +31-30-2535108. Fax: +31-30-2537725. E-mail: martynd@geo.uu.nl

occurrence of majoritic garnet relicts in the Otrøy peridotites has been described by Van Roermund & Drury (1998) and Van Roermund *et al.* (2000). Here we present new data on rock compositions in the Ugelvik peridotite. A new interpretation of the *P–T* history of the Otrøy peridotites and peridotites from kimberlite xenoliths is also presented. We compare possible *P–T* paths of cratonic peridotites with those predicted from numerical models of mantle convection and asthenosphere diapirism beneath a cratonic root (De Smet *et al.*, 1998, 1999, 2000). Finally, we discuss the implications of the numerical modelling results for the history and emplacement processes of deep upper-mantle rocks.

UPPER-MANTLE PERIDOTITES WITH MAJORITIC GARNET RELICTS

Orogenic peridotites, WGR, Norway

Many orogenic peridotite bodies occur in the WGR of Norway, which is a terrane of mainly Proterozoic basement rocks and infolded pre-Caledonian sediments reworked during the Caledonian orogeny. The dominant lithology is amphibolite-facies gneiss with bodies of higher-pressure eclogites and garnet peridotites (Krogh & Carswell, 1995). Breakdown products of majoritic garnet occur in garnet peridotites on the islands of Otrøy (Van Roermund & Drury, 1998), Flemsøy and Fjortøft (Terry *et al.*, 1999). Published isotope data from WGR peridotites suggest an age of depletion around 2·5–3·0 Ga whereas Sm–Nd dates range from early Proterozoic for early mineral assemblages to Caledonian ages for some recrystallized assemblages (Jamtveit *et al.*, 1991; Brueckner & Medaris, 1998).

The Otrøy peridotites have a clear compositional banding (Carswell, 1968; Van Roermund *et al.*, 2000) with bands of cpx-bearing garnet harzburgite (with minor lherzolites), garnet harzburgite, garnet-free harzburgite and dunites. Interlayered with the peridotites are lenses and layers of pyroxenites, garnet- and pyroxene-rich peridotites (Carswell, 1968, 1973) and some garnetites. The average composition of the Ugelvik body is harzburgite to dunite (Van Roermund *et al.*, 2000). The Raudhaugene body has less dunite and possibly more lherzolite than Ugelvik. The results from a detailed mapping study of the metre-scale average compositions in the eastern part of the Ugelvik peridotite are shown in Fig. 1. Compositional variations occur in a systematic and symmetric sequence of fertile to depleted compositions of cpx harzburgite, cpx-free harzburgite, opx dunite and dunite (Fig. 1).

Data on mineral and whole-rock chemistry from Carswell (1968, and unpublished data) are presented in Figs 2 and 3. Otrøy peridotites commonly have high modal olivine (75–95%) and high Fo (92–94) olivine (Medaris, 1984; Carswell, 1986; Van Roermund *et al.*, 2000). In terms of olivine composition and modal olivine (Fig. 2) the dominant Otrøy compositions are similar to some cratonic xenoliths (Bernstein *et al.*, 1998; McDonough & Rudnick, 1998; MacKensie & Canil, 1999; Schmidberger & Francis, 1999) and some Phanerozoic peridotites from supra-subduction settings (Bonetti & Micheal, 1989; Menzies, 1990; Bernstein *et al.*, 1998). Data for whole-rock chemistry (Fig. 3) show that the dominant depleted Otrøy rocks are similar to low-SiO_2 Kaapvaal xenoliths and Wiedemann Fjord xenoliths (Bernstein *et al.*, 1998). Compared with most Kaapvaal rocks, however, the Otrøy peridotites have lower whole-rock SiO_2 and modal orthopyroxene. Brueckner & Medaris (1998) showed that garnets in WGR peridotites have similar compositions to garnets from Precambrian cratonic xenoliths.

The Otrøy peridotites are similar to kimberlite xenoliths, as first emphasized by Carswell (1968). Both rock suites are dominated by depleted compositions and have an equigranular olivine microstructure. The *P–T* conditions estimated from mineral chemistry in kimberlite xenoliths define a cratonic array (Nixon & Boyd, 1973). The most recent *P–T* estimates (Brueckner & Medaris, 1998), for nine WGR peridotite bodies, fall along a similar array from 805°C and 3·4 GPa to 975°C and 5·4 GPa (Fig. 4). Megacrysts occur in both rock suites. At Otrøy garnet and olivine megacrysts occur as porphyroclasts in the peridotites whereas orthopyroxene megacrysts occur in websterite layers. Compared with the Kaapvaal xenoliths the Otrøy peridotites show a lack of hot sheared peridotites, lower modal orthopyroxene and overprinting of lower-pressure metamorphic reactions.

Brueckner & Medaris (1998) have shown that the Norwegian peridotites represent fragments of Precambrian cratonic lithosphere, which was present in a static cold environment a long time before being incorporated into the Caledonian orogeny. They concluded that the WGR peridotites are an 'excellent example of cold, melt depleted, buoyant lithosphere of the type that would be expected beneath the Baltic or Laurentian shield prior to Caledonian collision'. As noted by Brueckner & Medaris (1998) and Jamtveit *et al.* (1991), age data from WGR peridotites and crustal rocks indicate that this portion of continental lithosphere was possibly first formed in the Archaean and was later possibly involved in two Proterozoic orogenies and an episode of Mid-Proterozoic anorogenic magmatism.

P–T history of WGR peridotites

Van Roermund & Drury (1998) suggested that the *P–T* path of the Otrøy peridotites involves two main stages:

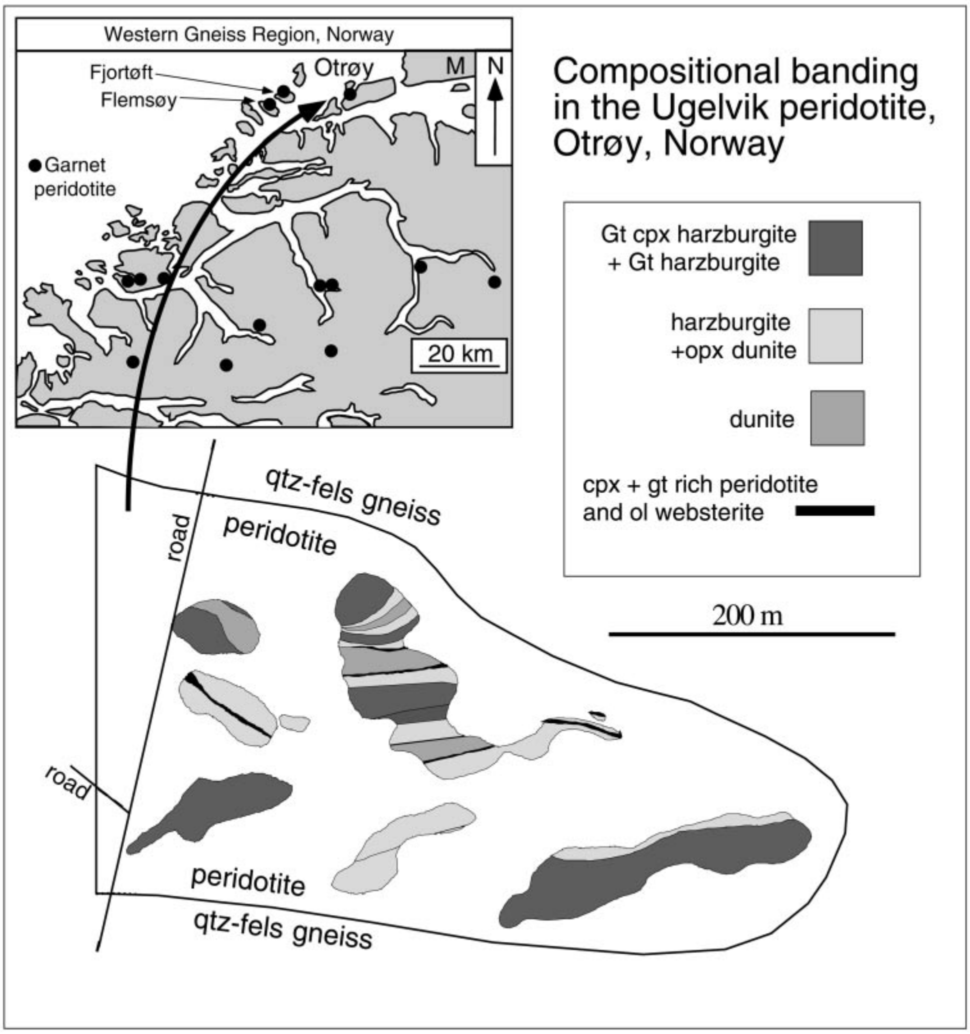

Fig. 1. Map of average composition in the eastern part of the Ugelvik peridotite. (Note the systematic sequence of compositional bands from fertile to depleted compositions.) Inset map shows the location of the Ugelvik peridotite and other garnet peridotites in the Western Gniess Region, Norway. M marks the location of the city Molde.

(1) adiabatic ascent from the stability field of majoritic garnet to the stability field of high-Al–Ca orthopyroxene (Carswell, 1973); (2) cooling to 800°C at pressures around 3 GPa. The stability field estimated for the high-Ca–Al orthopyroxene depends on the proportion of primary and exsolved garnet in the megacrystal orthopyroxene within the garnet websterite lens reported by Carswell (1973). Similar garnet peridotites and exsolved megacrystal orthopyroxene-dominant garnet websterite occur on the island of Fjortøft close to Otrøy (Terry *et al.*, 1999). The Fjortøft garnet websterite contains interstitial garnet with pyroxene exsolution lamellae between the orthopyroxene megacrysts with their internal exsolved garnet and clinopyroxene. This demonstrates that the high-Al–Ca orthopyroxenes were stable with majoritic garnet (Terry *et al.*, 1999). The *P*–*T* conditions for an assemblage of high-Al–Ca opx (4–3% Al_2O_3) and majoritic garnet (with 1–3% pyroxene exsolution) range from 3·4 GPa and 1490°C (Terry *et al.*, 1999) to 4·5 GPa and 1600°C based on the *P*–*T* grid of Fig. 4. It is not clear if the Otrøy high-Ca–Al megacrystal orthopyroxene was stable with majoritic garnet. Hence a range of *P*–*T* conditions are possible (Fig. 4) ranging from minimum conditions of around 2·7 GPa and 1350°C (point 1a in Fig. 4) to conditions of 4·5 GPa and 1600°C (point 1b in Fig. 4).

Megacrystal garnets containing pyroxene exsolution lamellae occur in the Otrøy peridotites as centimetre-scale aggregates and single grains. Some large garnets are associated with clinopyroxene (Carswell, 1973) although most garnets investigated by Van Roermund *et al.* (2001) contain interstitial orthopyroxene and inclusions of

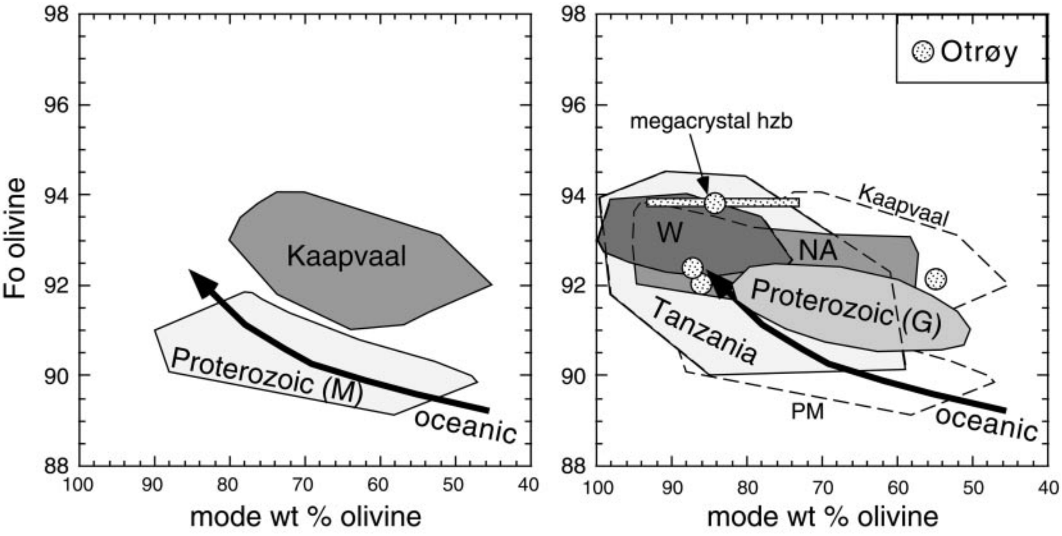

Fig. 2. Plot of olivine Fo content against modal olivine for Otrøy peridotites and other mantle samples. Left-hand plot shows original data for Archean Kaapvaal xenoliths and the oceanic trend from Boyd (1989) and some Proterozoic xenoliths (M) from Menzies (1990). Right-hand plot shows a selection of more recent data including: W, Wiedeman Fjord xenoliths (Bernstein *et al.*, 1998); NA, North American craton (MacKensie & Canil, 1999; Schmidberger & Francis, 1999); Tanzania craton (McDonough & Rudnick, 1998); (G), Proterozoic xenoliths (Griffin *et al.*, 1998). The point for megacrystal harzburgite from Otrøy is an estimated matrix composition based on field observations and composition of olivine inclusions in megacrystal garnets (Van Roermund *et al.*, 2000).

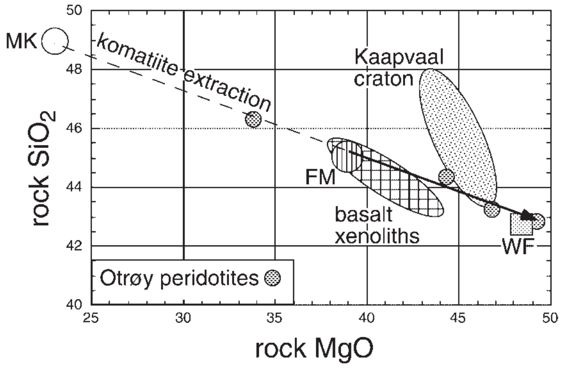

Fig. 3. Plot of whole-rock SiO_2 against MgO for Otrøy peridotites (Carswell, 1968) compared with other mantle samples. Kaapvaal xenoliths and basalt xenoliths after Takahashi (1990). FM, fertile mantle composition; WF, average composition of Wiedeman Fjord xenoliths; MK, Munro komatiite composition after Bernstein *et al.* (1998). The Otrøy data plot on a trend that is consistent with extraction of MK komatiite from a fertile mantle source.

orthopyroxene, subordinate olivine and minor amounts of cpx. The large majoritic garnet relicts in the peridotites could be porphyroclasts from a coarse early assemblage or they may have been formed from distributed melt segregations or disrupted websterite layers in the peridotite. Aggregates of garnet and clinopyroxene in otherwise highly depleted peridotites may be derived from some form of melt segregation whereas many garnet aggregates have compositions consistent with an origin as porphyroclasts. If the interstitial orthopyroxene and the orthopyroxene inclusions in the garnet aggregates formed by exsolution then original pressures of more than 6·5–8 GPa are implied, depending on temperature (Van Roermund *et al.*, 2001).

Extremely high temperatures of 1350–1600°C at depths of 80–130 km, suggestive of asthenosphere upwelling, are based on the stability of high-Al–Ca megacrystal orthopyroxene, which occurs in a discrete garnet websterite lens within the peridotites (Carswell, 1973). The *P–T* conditions inferred from a bulk integrated analysis of the exsolved megacrystal orthopyroxene given by Carswell (1973) provide a minimum estimate for the potential temperature of the upwelling mantle. The Otrøy peridotites could be derived from the upwelling deep mantle and possible *P–T* paths (a and b) are shown in Fig. 4. The original megacrystal orthopyroxenites probably formed by fractional crystallization from an intruding melt so the peridotites may not have experienced temperatures as high as the pyroxenites. The coarse exsolution microstructure in the orthopyroxene megacrysts (Carswell, 1973) suggests a slow cooling rate consistent with a small temperature difference of <200°C between the orthopyroxenite 'intrusion' and surrounding peridotite (Sautter & Fabriès, 1990). If the peridotites and pyroxenites had different *P–T* paths then it is possible that the peridotites could have been derived from deep lithospheric mantle (at 180–200 km) entrained and heated by upwelling asthenosphere (path c, Fig. 4).

The depleted composition of the Otrøy peridotites implies extensive melting and a substantial supersolidus *P–T* path at some stage in their history. Bernstein *et al.* (1998) concluded that such compositions (Fig. 3) can

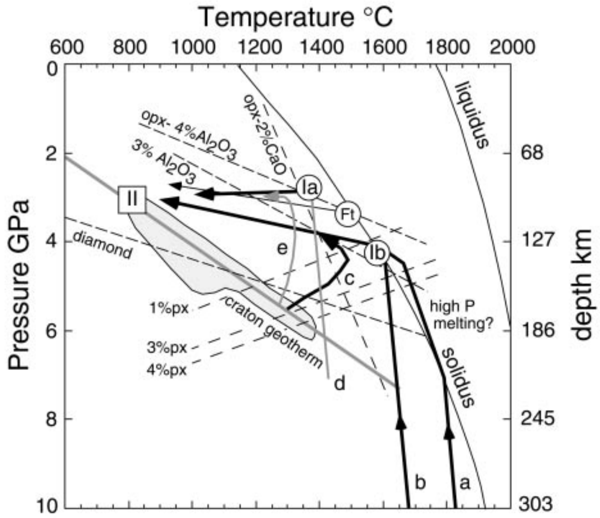

Fig. 4. *P–T* paths for Otrøy peridotites. The shaded area is the range of *P–T* estimates from mineral chemistry for WGR and kimberlite xenoliths. Points Ia and Ib show possible conditions for high-Al–Ca orthopyroxene. Majoritic garnet with 1–3% dissolved pyroxene is stable with high-Al–Ca orthopyroxene containing 3–4% Al_2O_3 at point Ib. Point Ft shows conditions for the Fjortøft megacrystal orthopyroxene (Terry *et al.*, 1999). *P–T* path (a) is the most simple path that fits all available data. Adiabatic decompression occurs with high-pressure melting to point Ib. Predominant cooling with some decompression occurs to point II along a cratonic geotherm. In path (b) adiabatic decompression occurs at lower temperature with minor high-pressure melting. In path (c) depleted lithospheric peridotites are heated and entrained by upwelling asthenosphere with crystallization of melts derived from the asthenosphere at Ib. Paths (d) and (e) are equivalent to paths (b) and (c), respectively, with decompression to point Ia. The contours for pyroxene content of majoritic garnet are based on experimental data for natural compositions (see Van Roermund *et al.*, 2001).

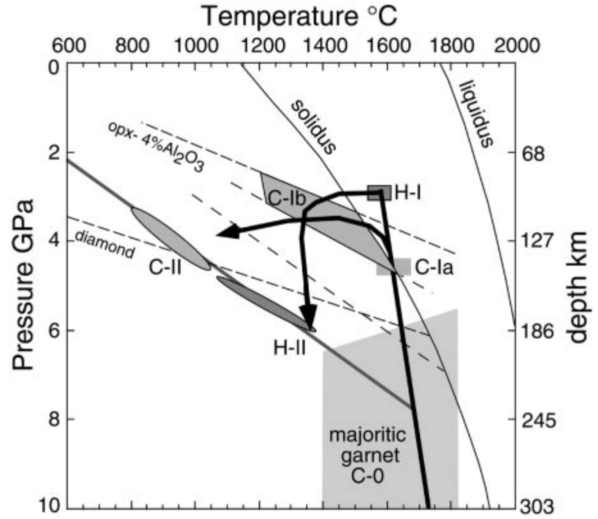

Fig. 5. *P–T* path for kimberlite xenoliths. *P–T* conditions estimated for majoritic garnet C-0 (Sautter *et al.*, 1991), high-Al–Ca orthopyroxene, C-Ib from Cox *et al.* (1987), C-Ia and H-I from Canil (1991) and from mineral chemistry of minerals (C-II and H-II) (e.g. Nixon & Boyd, 1973) suggest a history of adiabatic decompression followed by cooling from C-Ia or C-Ib to C-II for cold undeformed xenoliths and a history of adiabatic decompression followed by cooling and increasing pressure from point HI to H-II for the hot deformed xenoliths (Canil, 1991).

be produced either by dissolution of pyroxene from previously depleted peridotites, perhaps in an arc setting, or by extraction of Munro-type komatiite at pressures of 2–3 GPa. The compositional data (Fig. 3) of the depleted Otrøy peridotites lie on a trend consistent with komatiite extraction. Extensive melting at <4·5 GPa, however, would result in the complete consumption of garnet (Herzberg & O'Hara, 1998; Walter, 1998) and majoritic garnet porphyroclasts would not be preserved in the residual peridotite.

Melting of the Otrøy rocks could have occurred during emplacement into Proterozoic lithosphere (path a, Fig. 4). The crystallization of megacrystal orthopyroxenites could mark the end of melting at 3·4–5 GPa during upwelling from the deeper mantle. The preservation of centimetre-scale relict majoritic garnet porphyroclasts is possible if melting occurred above 4·5 GPa (Walter, 1998). Alternatively, the depleted compositions and preservation of relict majoritic garnet porphyroclasts could be explained by a more complex history of early shallow melting and tectonic transport to the deep upper mantle, followed by upwelling and emplacement into Proterozoic lithosphere (path b or c, Fig. 4).

P–T history of kimberlite xenoliths

Many studies (e.g. Nixon & Boyd, 1973) have used the *P–T* estimates from kimberlite xenoliths to estimate the geotherm at the time of kimberlite eruption. The earlier *P–T* history can also be deduced (Fig. 5) from the reconstruction of early mineral compositions based on exsolution relationships. Xenoliths with breakdown products of majoritic garnet (Sautter *et al.*, 1991) imply original depths in the deep upper mantle to transition zone. Cox *et al.* (1987) and Boyd & Mertzman (1987) presented evidence that garnet and clinopyroxene in both cold undeformed and hot deformed xenoliths exsolved from a high-Ca–Al pyroxene precursor, implying cooling from temperatures of 1200–1600°C down to 800–1000°C at depths around 125–150 km. Eclogite xenoliths containing megacrystal pyroxene grains with exsolution provide independent evidence for this cooling (Lappin & Dawson, 1975; Harte & Gurney, 1975). *P–T* paths can be inferred for the cold undeformed kimberlite xenoliths (Fig. 5) with high-temperature decompression from the stability field of majoritic garnet to the stability field of the high-Ca–Al pyroxenes followed by dominant cooling from 1200–1600°C down to a normal cratonic geotherm (Fig. 5). For hot sheared kimberlite xenoliths a *P–T* path involving cooling and increasing pressure is implied (Fig. 5) (Cox *et al.*, 1987; Canil, 1991).

The depleted compositions of kimberlite xenoliths suggest that extensive melting occurred at some time in their history. Melting and depletion could have occurred during asthenosphere upwelling into cratonic lithosphere or in an earlier stage of a more complex history involving early shallow melting, tectonic transport to deeper levels and finally upwelling with limited high-pressure melting during emplacement of the peridotites into cratonic lithosphere. Kelemen *et al.* (1998) have argued that a correlation between CaO and Yb contents in cratonic garnet peridotites implies that most melting occurred at pressures <3 GPa, suggesting that a multi-stage history may be applicable to kimberlite xenoliths.

The *P–T* paths derived for the Otrøy peridotites and kimberlite xenoliths are qualitatively consistent with upwelling of hot asthenosphere to lithospheric depths (Kornprobst, 1969; Nicolas, 1986). This type of *P–T* path has also been obtained for asthenosphere diapirs in a numerical model for continental lithosphere formation (De Smet *et al.*, 2000). We now describe the results from the modelling study of De Smet *et al.* (1998, 1999, 2000).

NUMERICAL THERMOCHEMICAL CONVECTION MODELS

De Smet *et al.* (1998, 1999, 2000) studied the evolution of the continental lithosphere using a thermochemical convection model of the upper mantle below stable continental crust. The model considers only sub-continental cratonic mantle and does not include the effects of subduction. The lower mantle is treated as a heat reservoir with no material transfer from the lower mantle to upper mantle via plumes or mantle overturns. The key petrological features are (1) the effect of melting on peridotite density and (2) a simplified phase diagram with linear solidus and liquidus, which is a good approximation at depths <150 km but less realistic at deeper levels. Use of a linear solidus reduces the amount of deep melting and the extent of mantle differentiation (De Smet *et al.*, 1999). Partial melting and melt extraction results in a density decrease of the residual peridotite (O'Hara, 1975); a relationship based on Jordan (1979) was used. The results show that a depleted lithosphere 150–200 km thick forms quickly, in 50–100 my, and remains stable for billions of years (De Smet *et al.*, 1998), which is consistent with evidence from Archaean cratons (Richardson *et al.*, 1984; Boyd *et al.*, 1985; Menzies *et al.*, 1987; Pearson, 1999). Subsequent lithosphere growth occurs by accretion of small diapirs, of 50–100 km diameter (Fig. 6), which originate from instabilities near the base of the cratonic root (De Smet *et al.*, 1998). Material can rise from the transition zone in an upwelling limb of a larger-scale mantle convection cell, become included in a small-scale diapir and then rise into the lithospheric root. As the diapirs rise, melting occurs and continues until the diapirs stop at a depth of 60–100 km (Fig. 6) beneath the high-viscosity mechanical boundary layer (MBL). Diapirs form as relatively small-scale instabilities near the base of the lithosphere. They do not originate as instabilities from a hot boundary layer at the base of the upper mantle. Intrusion of diapirs results in local, small-scale convection in the lower part of the cratonic lithosphere. This small-scale circulation stretches and attenuates rock volumes with different depletion and produces a compositional banding in the lithosphere (De Smet *et al.*, 2000).

In a model run for a simulated period of 4 by, three episodes of craton growth occurred (De Smet *et al.*, 2000). Lithosphere growth by episodes of asthenosphere diapirism occurred only in the first 3 by, when the horizontally averaged mantle temperature was >1550°C.

P–T–t paths for individual tracers in the model (De Smet *et al.*, 2000) are compared in Fig. 7 with the *P–T* estimates for cratonic peridotites. The *P–T* paths from the numerical model are for tracer particles in diapirs from three different stages of craton growth. These tracers started in the deep upper mantle. The paths show adiabatic decompression during ascent to the base of the lithosphere and during intrusion of the diapir into the lithosphere. Approximately isobaric cooling occurs once the diapir stagnates below the high-viscosity MBL at depths of 60–100 km and cools to the ambient cratonic geotherm. Some parts of diapirs (or earlier hotter diapirs) can become involved in the small-scale circulation in the lower part of the thermochemical lithosphere and descend to the base of the lithosphere. One tracer shown in Fig. 7 rose to 75 km but ended up at depths of 150 km. De Smet *et al.* (2000) have shown that continued circulation in the root can produce a remarkable spiral *P–T* path with episodes of recurrent melting.

DISCUSSION

The subsolidus *P–T* paths deduced for kimberlite xenoliths and some of the possible paths (paths a and b, Fig. 4) for the Otrøy peridotites are similar to *P–T* paths obtained from the numerical model (Fig. 7). Thus, the *P–T* paths of deep upper-mantle peridotites are consistent with transport to shallow depths by convection and asthenosphere diapirism in a hot upper mantle. As there are limited constraints on the timing and conditions of melting in the Otrøy peridotites the *P–T* paths are also consistent with diapiric upwelling of previously depleted mantle from the transition zone (e.g. Ringwood, 1989) or lower mantle (Haggerty, 1994).

Very high potential temperatures for melting or mantle upwelling are often attributed to mantle plumes. It is

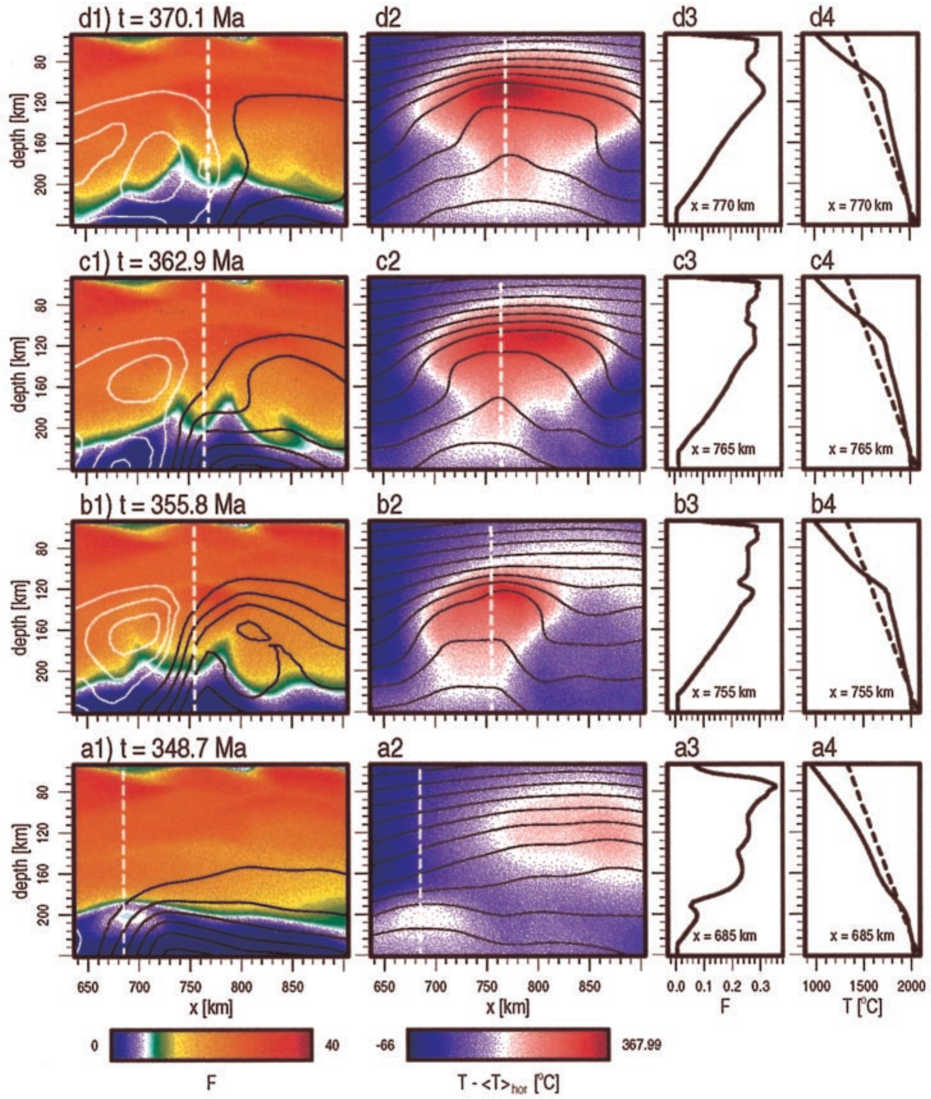

Fig. 6. Results from numerical thermo-convection model showing intrusion of asthenosphere diapir into cratonic lithosphere. a1–d1 show evolution of degree of depletion with colours representing depletions from 0 to 40%. Streamlines in a1–d1 are selected contours of the instantaneous stream function: black lines and white lines represent clockwise and counter-clockwise flow, respectively. a2–d2 show the evolution of the thermal field. The isotherms have an increment of 110°C, and the colours show the deviation of the temperature from the horizontally averaged temperature. a3–d3 show vertical cross-sections of degree of depletion along the dotted white line in a1–d1. a4–d4 show cross-sections of the temperature variation through the diapir centre.

important to distinguish between diapiric instabilities, which form close to the base of the lithosphere, and plumes, which originate as instabilities from thermal boundary layers deeper in the mantle. The high temperatures inferred for early mineral assemblages in cratonic peridotites (Figs 4 and 5) can be explained either by asthenosphere diapirism in a hot upper mantle or possibly by episodes of plume activity (Haggerty & Sautter, 1990; Herzberg, 1993; Haggerty, 1994). A hot upper mantle may occur beneath cratons in the Precambrian (De Smet *et al.*, 1998) or may arise from mantle overturn events (Tackley *et al.*, 1993; Griffin *et al.*, 1998).

The model *P–T* paths have a substantial supersolidus path with melting over a large pressure range. *P–T* paths like this may be possible for the WGR peridotites but extensive deep melting may be inconsistent with the CaO–Yb correlation in the kimberlite xenoliths (Kelemen *et al.*, 1998). As shown in Figs 4 and 5 cratonic peridotites may have *P–T* paths with limited melting during upwelling. If this is the case then earlier melting followed by

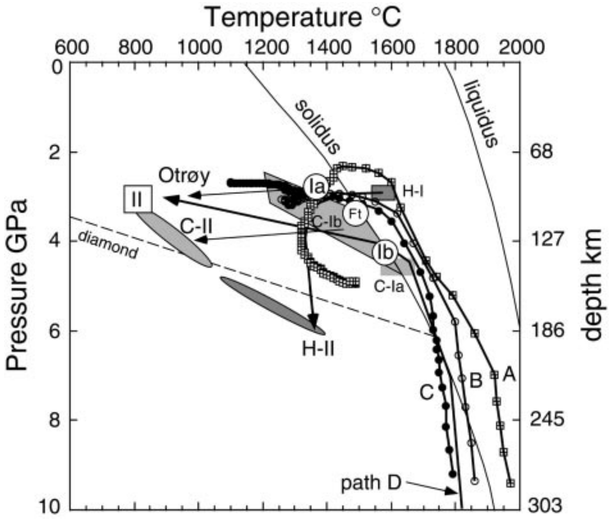

Fig. 7. P–T paths from the numerical thermo-convection model for tracer points in three asthenosphere diapirs (A, B and C). Time period between data points is 1 my. Also shown for comparison are the P–T conditions estimated for mineral assemblages in the Otrøy peridotites (Ia, Ib and II), Fjortøft peridotites (Ft) (Terry *et al.*, 1999) cold undeformed kimberlite xenoliths (C-Ia, C-Ib, C-II) and hot deformed (H-I, H-II) kimberlite xenoliths. Path D shows the simplest P–T path for Otrøy that fits all available data. Other more complex histories are also possible (Fig. 4).

tectonic transport to deeper levels is required before the upwelling event (e.g. Ringwood, 1989). The dynamics of upwelling diapirs derived from deep thermochemical boundary layers may be very different from that of diapirs forming near the base of the cratonic lithosphere.

The P–T path for hot deformed kimberlite xenoliths suggested by Canil (1991) is similar to model P–T paths where material becomes involved in small-scale convection in the cratonic root. Thus this type of P–T path is plausible and can be explained by small-scale convection. It is uncertain, however, if the hot deformed xenoliths have such a P–T history. The stage of equilibrium at high temperatures and shallow depths (3 GPa) is based on evidence that the garnet and pyroxene in these xenoliths were exsolved from a high-Al–Ca opx precursor (Cox *et al.*, 1987). In some sheared xenoliths, however, 40–70% of the garnet was formed during later metasomatism (Griffin *et al.*, 1989; Smith & Boyd, 1989). Boyd & Mertzman (1987) and Walter (1998) have shown that the compositions of hot sheared xenoliths are consistent with melting at relatively low to moderate pressures, suggesting that some form of tectonic transport to deeper levels is required.

In the numerical models small-scale convection in the lower part of the cratonic root is active during episodes of craton growth and diapir intrusion (Fig. 6). Stirring produced by convection in the craton root will modify the simple variation of depletion with depth expected from polybaric melting (Kelemen *et al.*, 1998). The variation of peridotite depletion with depth derived from the numerical models shows an overall trend of decreasing depletion with depth (Fig. 6) but on a smaller scale the compositional variation is complex (De Smet *et al.*, 1998, 2000). The compositional banding in the models is produced by stretching of diapir-scale (10–100 km diameter) heterogeneities produced by variations in melt extraction. Studies on stirring and mixing in fluid flows show that outcrop-scale compositional banding in cratonic peridotites (Fig. 1) can be formed by convective stirring of heterogeneities in the craton root (Allègre & Turcotte, 1986; Kellog & Turcotte, 1986).

Small-scale convection in the cratonic root can account for the transport of material to deeper levels in the cratonic root without invoking subduction. Within one episode of craton growth, cratonic peridotites can be involved in several stages of diapirism, upwelling, melting and recirculation in the dynamic cratonic root. Thus, melting and depletion of a peridotite body may occur in an earlier stage of evolution than the upwelling event that resulted in the final emplacement in the lithosphere. Small-scale convection can transport material to deeper levels but a subduction-like process is needed to transport near-surface material to the deep upper mantle and transition zone. Eclogite xenoliths in kimberlites may be derived from oceanic crust (e.g. Jagoutz *et al.*, 1984; Jacob & Foley, 1999). In addition, some eclogite xenoliths bear evidence for residence at transition zone depth (Haggerty & Sautter, 1990). Other eclogites contain high-temperature exsolution microstructures (Harte & Gurney, 1975), suggesting high temperatures during lithosphere emplacement. The combined evidence from eclogites is consistent with a shallow origin and deep tectonic transport, followed by high-temperature upwelling and emplacement into cratonic lithosphere (MacDougall & Haggerty, 1999).

In the numerical models of De Smet *et al.* (1998, 1999, 2000) episodes of asthenosphere diapirism and emplacement of deep upper-mantle material occurred in the simulated Precambrian when the potential temperature is above 1550°C. Deep mantle rocks may also be emplaced in the lithosphere in the Phanerozoic by upwelling of previously depleted material from the transition zone (Ringwood, 1989; Ringwood *et al.*, 1992) or from the core–mantle boundary (Haggerty, 1994). In a study on Nd and Sr isotopes, MacDougall & Haggerty (1999) found evidence that deep mantle rocks were emplaced into the cratonic lithosphere over time scales of many hundreds of million years during episodes of plume- or kimberlite-related magmatism in the Precambrian and Phanerozoic.

CONCLUSIONS

(1) In terms of mineral and whole-rock chemistry the Otrøy orogenic peridotites in the Western Gneiss Region of Norway are similar to Precambrian cratonic xenoliths and Phanerozoic supra-subduction-zone peridotites.

(2) Mineral compositions and reconstructed early mineral compositions in the Otrøy peridotites and kimberlite xenoliths suggest a P–T path with high-temperature decompression from depths of >200 km to 100–150 km, followed by cooling to conditions on a cratonic geotherm.

(3) Outcrop-scale compositional banding in craton peridotites can be produced by small-scale convection associated with diapirism in the deeper, low-viscosity part of the thermochemically defined cratonic lithosphere.

(4) Complex P–T histories and multi-stage metamorphic–igneous histories can be produced during craton growth by asthenosphere diapirism in a hot upper mantle.

(5) P–T paths predicted from models of asthenosphere diapirism are consistent with the subsolidus P–T history deduced for the Otrøy orogenic peridotites and Kaapvaal kimberlite xenoliths.

ACKNOWLEDGEMENTS

This work was supported by an NWO (Netherlands Organization for Scientific Research) PIONIER subsidy. Martin Menzies and two anonymous referees are thanked for comprehensive and constructive reviews.

REFERENCES

Allègre, C. J. & Turcotte, D. L. (1986). Implications of a two-component marble-cake mantle. *Nature* **323**, 123–127.

Bernstein, S., Kelemen, P. B. & Kent Brooks, C. (1998). Depleted spinel harzburgite xenoliths in Tertiary dykes from East Greenland: restite from high degree melting. *Earth and Planetary Science Letters* **154**, 221–235.

Bonetti, E. & Micheal, P. J. (1989). Mantle peridotites from continental rifts to ocean basins to subduction zones. *Earth and Planetary Science Letters* **9**, 297–311.

Boyd, F. R. (1989). Compositional distinction between oceanic and cratonic lithosphere. *Earth and Planetary Science Letters* **9**, 15–26.

Boyd, F. R. & Mertzman, S. A. (1987). Composition and structure of the Kaapvaal lithosphere, southern Africa. In: Mysen, B. O. (ed.) *Magmatic Processes: Physicochemical Principles. Geochemical Society, Special Publication* **1**, 13–24.

Boyd, F. R., Gurney, J. J. & Richardson, S. H. (1985). Evidence for a 150–200 km thick Archaean lithosphere from diamond inclusion barometry. *Nature* **315**, 387–389.

Bozhilov, K. N., Green, H. W., II & Dobrzhinetskaya, L. (1999). Clinoenstatite in Alpe Arami peridotite: additional evidence of very high pressure. *Science* **284**, 128–132.

Brueckner, H. K. & Medaris, L. G. (1998). A tale of two orogens: the contrasting T–P–t history and geochemical evolution of mantle in high and ultra-high pressure metamorphic terranes of the Norwegian Caledonides and the Czech Variscides. *Schweizerische Mineralogische und Petrographische Mitteilungen* **78**, 293–307.

Canil, D. (1991). Experimental evidence for the exsolution of cratonic peridotite from high temperature harzburgite. *Earth and Planetary Science Letters* **106**, 64–72.

Carswell, D. A. (1968). Possible primary upper mantle peridotite in Norwegian basal gneiss. *Lithos* **1**, 322–355.

Carswell, D. A. (1973). Garnet pyroxenite lens within Ugelvik layered garnet peridotite. *Earth and Planetary Science Letters* **20**, 347–352.

Carswell, D. A. (1986). The metamorphic evolution of Mg–Cr type Norwegian garnet peridotites. *Lithos* **19**, 279–297.

Cox, K. G., Smith, M. R. & Beswetherick, S. (1987). Textural studies of garnet lherzolites: evidence of exsolution origin from high temperature harzburgites. In: Nixon, P. H. (ed.) *Mantle Xenoliths*. New York: John Wiley, pp. 537–550.

De Smet, J. H., van den Berg, A. P. & Vlaar, N. J. (1998). Stability and growth of continental shields in mantle convection models including recurrent melt production. *Tectonophysics* **296**, 15–29.

De Smet, J. H., van den Berg, A. P. & Vlaar, N. J. (1999). Evolution of continental roots in numerical thermo-chemical mantle convection models including differentiation by partial melting. *Lithos* **48**, 153–170.

De Smet, J. H., van den Berg, A. P. & Vlaar, N. J. (2000). Early formation and long-term stability of continents resulting from decompression melting in a convecting mantle. *Tectonophysics* **322**, 19–33.

Dobrzhinetskaya, L., Green, H. W. & Wang, S. (1996). Alpe Arami: a peridotite massif from depths of more than 300 km. *Science* **271**, 1841–1845.

Griffin, W. L., Smith, D., Boyd, F. R., Cousens, D. R., Ryan, C. G., Sie, S. H. & Suter, G. F. (1989). Trace-element zoning in garnets from sheared xenoliths. *Geochimica et Cosmochimica Acta* **53**, 561–567.

Griffin, W. L., O'Reilly, S. Y., Ryan, C. G., Gaul, O. & Ionov, D. A. (1998). Secular variation in the composition of subcontinental lithospheric mantle: geophysical and geodynamic implications. In: Braun, J., Dooley, J., Goleby, B., van der Hilst, R. & Klootwijk, C. (eds) *Structure and Evolution of the Australian Continent. American Geophysical Union, Geodynamics Series* **26**, 1–26.

Haggerty, S. E. (1994). Superkimberlites: a geodynamic diamond window to the Earth's core. *Earth and Planetary Science Letters* **122**, 57–69.

Haggerty, S. E. & Sautter, V. (1990). Ultradeep (greater than 300 km) ultramafic upper mantle xenoliths. *Science* **248**, 993–996.

Harte, B. & Gurney, J. J. (1975). Evolution of clinopyroxene and garnet in an eclogite nodule from the Roberts Victor kimberlite pipe. *Physics and Chemistry of the Earth* **9**, 367–387.

Harte, B., Harris, J. W., Hutchinson, M. T., Watt, G. R. & Wilding, M. C. (1999). Lower mantle mineral associations in diamonds from São Luiz, Brazil. In: Fei, Y., Bertka, C. M. & Mysen, B. O. (eds) *Mantle Petrology: Field Observations and High Pressure Experimentation: a Tribute to Francis R. (Joe) Boyd. Geochemical Society, Special Publication* **6**, 125–153.

Herzberg, C. T. (1993). Lithospheric peridotites of the Kaapvaal craton. *Earth and Planetary Science Letters* **120**, 13–29.

Herzberg, C. (1995). Phase equilibria of common rocks in the crust and mantle. In: Ahrens, T. J. (ed.) *Rock Physics and Phase Relations. A Handbook of Physical Constants. American Geophysical Union Reference Shelf* **3**, 166–177.

Herzberg, C. & O'Hara, M. J. (1998). Phase equilibrium constraints on the origin of basalts, picrites, and komatiites. *Earth-Science Reviews* **44**, 39–79.

Jacob, D. E. & Foley, S. F. (1999). Evidence for Archean ocean crust with low high field strength element signature from diamondiferous eclogite xenoliths. *Lithos* **48**, 317–336.

Jagoutz, E., Dawson, J. B., Hoerness, S., Spettl, B. & Wänke, H. (1984). Anorthositic oceanic crust in the Archean Earth. *Proceedings of the 15th Lunar and Planetary Science Conference. Journal of Geophysical Research* **90** (Supplement), 395–396.

Jamtveit, B., Carswell, D. A. & Mearns, E. W. (1991). Chronology of the high-pressure metamorphism of Norwegian garnet peridotites/pyroxenites. *Journal of Metamorphic Geology* **9**, 1–15.

Jordan, T. H. (1979). Mineralogies, densities, and seismic velocities of garnet lherzolites and their geophysical implications. In: Boyd, F. R & Meyer, H. O. A. (eds) *The Mantle Sample: Inclusions in Kimberlites and other Volcanics*. Washington, DC: American Geophysical Union, pp. 1–14.

Kelemen, P. B., Hart, S. R. & Bernstein, S. (1998). Silica enrichment in the continental upper mantle via melt/rock reaction. *Earth and Planetary Science Letters* **164**, 387–406.

Kellog, L. H. & Turcotte, D. L. (1986). Homogenisation of the mantle by convective mixing and diffusion. *Earth and Planetary Science Letters* **81**, 371–378.

Kesson, S. E. & Fitz Gerald, J. D. (1991). Partitioning of MgO, FeO, NiO, MnO, Cr_2O_3, between magnesian silicate perovskite and magnesiowüstite: implications for the origin of inclusions in diamond and the composition of the lower mantle. *Earth and Planetary Science Letters* **111**, 229–240.

Kornprobst, J. (1969). Le massif ultrabasique des Beni Bouchera (Rif Interne, Maroc): étude des péridotites de haute température et de haute pression, et des pyroxénolites, à grenat ou sans grenat. *Contributions to Mineralogy and Petrology* **23**, 283–322.

Krogh, E. J. & Carswell, D. A. (1995). HP and UHP eclogites and garnet peridotites in the Scandinavian Caledonides. In: Coleman, R. G. & Wang, X. (eds) *Ultrahigh Pressure Metamorphism. Cambridge Topics in Petrology*. Cambridge: Cambridge University Press, pp. 244–298.

Lappin, M. A. & Dawson, J. B. (1975). Two Roberts Victor cumulate eclogites and their re-equilibration. *Physics and Chemistry of the Earth* **9**, 351–366.

MacDougall, J. D. & Haggerty, S. E. (1999). Ultradeep xenoliths from African kimberlites: Sr and Nd isotopic compositions suggest complex history. *Earth and Planetary Science Letters* **170**, 73–82.

MacKensie, J. M. & Canil, D. (1999). Composition and thermal evolution of cratonic mantle beneath the central Archean Slave Province, NWT, Canada. *Contributions to Mineralogy and Petrology* **134**, 313–324.

McDonough, W. F. & Rudnick, R. L. (1998). Mineralogy and composition of the upper mantle. In: Hemley, R. J. (ed.) *Ultrahigh-pressure Mineralogy. Mineralogical Society of America, Reviews in Mineralogy* **37**, 139–159.

Medaris, L. G. (1984). A geothermobarometric investigation of garnet peridotites in the Western Gneiss Region of Norway. *Contributions to Mineralogy and Petrology* **87**, 72–86.

Menzies, M., Rogers, N., Tindle, A. & Hawkesworth, C. (1987). Metasomatic and enrichment processes in lithospheric peridotites, an effect of asthenosphere–lithosphere interaction. In: Menzies, M. A. & Hawkesworth, C. J. (eds) *Mantle Metasomatism*. London: Academic Press, pp. 313–361.

Menzies, M. A. (1990). Archean, Proterozoic, and Phanerozoic lithosphere. In: Menzies, M. A. (ed.) *Continental Mantle*. Oxford: Oxford University Press, pp. 67–86.

Moore, R. O. & Gurney, J. J. (1985). Pyroxene solid solution in garnets included in diamonds. *Nature* **335**, 784–789.

Moore, R. O., Gurney, J. J., Griffin, W. L. & Shimizu, N. (1991). Ultrahigh pressure garnet inclusions in Monastery diamonds: trace element abundance patterns and conditions of origin. *European Journal of Mineralogy* **3**, 213–230.

Nicolas, A. (1986). Structure and petrology of peridotites: clues to their geodynamic environment. *Reviews of Geophysics* **24**, 875–895.

Nixon, P. H. & Boyd, F. R. (1973). Petrogenesis of the granular and sheared ultrabasic nodule suite in kimberlites. In: Nixon, P. H. (ed.) *Lesotho Kimberlites*. Meseru: Lesotho National Development Corporation, pp. 48–56.

O'Hara, M. J. (1975). Is there an Icelandic mantle plume? *Nature* **253**, 708–710.

Pearson, D. G. (1999). The age of continental roots. *Lithos* **48**, 171–194.

Pearson, D. G., Davies, G. R., Nixon, P. H. & Milledge, H. J. (1989). Graphitized diamonds from a peridotite massif in Morocco and implications for anomalous diamond occurrences. *Nature* **338**, 60–62.

Pfiffner, M. & Trommsdorff, V. (1998). The high pressure ultramafic–mafic–carbonate suite of Cima Lunga–Adula, Central Alps: excursions to Cima di Gagnone and Alpe Arami. *Schweizerische Mineralogische und Petrographische Mitteilungen* **78**, 337–354.

Richardson, S. H., Gurney, J. J., Erlank, A. J. & Harris, J. W. (1984). Origin of diamonds in old enriched mantle. *Nature* **310**, 198–202.

Ringwood, A. E. (1989). Constitution and evolution of the mantle. In: Ross, J., Jaques, A. L., Ferguson, J. *et al.* (eds) *Kimberlites and Related Rocks. Geological Society of America, Special Publication* **14**(1), 457–485.

Ringwood, A. E., Kesson, S. E., Hibberson, W. & Ware, N. (1992). Origin of kimberlites and related magmas. *Earth and Planetary Science Letters* **113**, 521–538.

Sautter, V. & Fabriès, J. (1990). Cooling kinetics of garnet websterites from the Freychinède orogenic lherzolite massif, French Pyrenees. *Contributions to Mineralogy and Petrology* **105**, 533–549.

Sautter, V., Haggerty, S. E. & Field, F. (1991). Ultradeep (>300 kilometres) ultramafic xenoliths: petrological evidence from the transition zone. *Science* **252**, 827–830.

Schmidberger, S. S. & Francis, D. (1999). Nature of the mantle roots beneath the North American craton: mantle xenolith evidence from Somerset Island kimberlites. *Lithos* **48**, 195–216.

Scott-Smith, B. H., Danchin, R. V., Harris, J. W. & Stracke, K. J. (1984). Kimberlites near Ororroo, South Australia. In: Kornprobst, J. (ed.) *Kimberlites I: Kimberlites and Related Rocks*. Amsterdam: Elsevier, pp. 121–142.

Smith, D. & Boyd, F. R. (1989). Compositional heterogeneities in minerals of sheared xenolith inclusions from African kimberlites. In: Ross, J., Jaques, A. L. , Ferguson, J. *et al.* (eds) *Kimberlites and Related Rocks. Geological Society of America, Special Publication* **14**(2), 709–724.

Tackley, P. J., Stevenson, D. J., Glazmaier, G. A. & Schubert, G. (1993). Effects of an endothermic phase transition at 670 km depth in a spherical model of convection in the Earth's mantle. *Nature* **361**, 699–704.

Takahashi, E. (1990). Speculations on the Archean mantle: missing link between komatiite and depleted garnet peridotite. *Journal of Geophysical Research* **95**, 15941–15954.

Terry, M. P., Robinson, P., Carswell, D. A. & Gasparik, T. (1999). Evidence for a Proterozoic mantle plume and a thermotectonic model for exhumation of garnet peridotites, Western Gneiss Region, Norway. *EOS Transactions, American Geophysical Union* **80**, S359–S360.

Van Roermund, H. L. M. & Drury, M. R. (1998). Ultra-high pressure (P >6 GPa) garnet peridotites in Western Norway: exhumation of mantle rocks from more than 185 km. *Terra Nova* **10**, 295–301.

Van Roermund, H. L. M., Drury, M. R., Barnhoorn, A. & de Ronde, A. (2000). Super-silicic garnet microstructures from an orogenic peridotite, evidence for an ultra-deep origin. *Journal of Metamorphic Geology* **18**, 135–147.

Van Roermund, H. L. M., Drury, M. R., Barnhoorn, A. & de Ronde, A. (2001). Relict majoritic garnet microstructures from ultra-deep orogenic peridotites in Western Norway. *Journal of Petrology* **42**, 117–130.

Walter, M. J. (1998). Melting of garnet peridotite and the origin of komatiite and depleted lithosphere. *Journal of Petrology* **39**, 29–60.